

Urban Heat Island Amplification Estimates on Global Warming Using an Albedo Model

Alec Feinberg

Key Words: Urban Heat Islands, Albedo Modeling, UHI Amplification Effects, Global Warming Causes and Amplification Effects, UHI Footprint, UHI Heat Dome, Cool Roofs, Sea Ice and Moisture Feedbacks

Abstract In this paper we provide nominal and worst case estimates of radiative forcing due to UHI effect (including urban areas) using a Weighted Amplification Albedo Solar Urbanization (WAASU) Model. This is done with the aid of reported findings from UHI footprint and heat dome studies that simplified estimates for UHI amplification factors. Using this method, we find between 1.5 and 21% of global warming may be due to the UHI effect (with urban areas). These values may increase in terms of the root-cause assessment 4.2 and 38% when climate feedback values are estimated. These large variations are due to urbanized area and UHI area amplification factor uncertainties. However, the model showed consistent estimates of about 0.1 (W/m²)/°K/%Normalized Area for the urbanized feedback value. The model is additionally used to quantify an assessment of sea ice feedback warming. Results provide insight into the UHI area effects from a new perspective and illustrates that one needs to take into account effective UHI amplification factors when assessing UHI's warming effect on a global scale. Lastly, such effects likely show a persuasive argument for the need of world-wide UHI albedo goals.

1 Introduction

It is concerning that there are so few UHI publications recently on their possible influences to global warming. Part of the motivation for this paper is to illustrate the continual need for more up-to-date related studies including UHI amplification effects (that include their urban areas) as will be discussed in this paper. The subject of UHI effect having significant contributions to global warming is very important and should remain so. The topic has a controversial history. One such paper, McKittrick and Michaels (2007) found that the net warming bias at the global level may explain as much as half the observed land-based warming. This study was criticized by Schmidt (2009) and defended for a period of about 10 years by Mckittrick (see McKittrick Website). Other authors have also found significance (Zhao, 1991; Feddema et al., 2005; Ren et al., 2007, 2008; Jones et al., 2008; Stone, 2009; Zhao, 2011; Yang et al. 2011, and Haung et al. 2015). These studies used land-based temperature station data to make assessments. Although the studies have all found global warming UHI significance with different assessments, they have yet to influence the IPCC enough to necessitate albedo recommendations in their many reports and meetings like the CO₂ effort. This is important because we feel the IPCC's should be more proactive in helping the global community recognizing the need for UHI albedo guidelines. Although the IPCC have provided reports on UHIs including health related issues, the response to their reports does not appear to be effective on the global scale compared with the on-going CO₂ effort.

The contention that UHI effects are basically only of local significance is most likely related to urban area estimates. For example, IPCC (Satterthwaite et. al. 2014) AR5 report references Schneider et al. (2009) study that resulted in urban coverage of 0.148% of the Earth (Table 1). This seemingly small area tends to dismiss the contention that UHI effect can play a large scale role in global warming. Furthermore, estimates of how much of land has been urbanized vary widely in the literature and this is in part due to the definition of what is urban and the datasets used. Although, such estimates are important for environmental studies, obtaining true estimates for the small urbanized area relative to the total land is apparently very difficult. This is compounded by the fact that there is a significant difference in how groups define the term 'urban'. Thus, urbanized surface area land approximations vary widely and most are obtained with satellite measurements sometimes supplemented in some way with census data. Table 1 captures the variations from some papers that are of interest.

Table 1. Urbanization area extent estimates from various sources

Percent of Land	Percent of Earth	References
2.7	0.783	GRUMP, 2005 - using NASA satellite light studies based on 2004 data and supplemented with census data
1%	0.29	NASA, 2000; Galka, 2016 – from satellite data
0.51	0.148	Schneider et al. 2009 - based on 2000-2001 data and referenced in the IPCC report (Satterthwaite, 2014)
0.5%	0.145	Zhou 2015 - based on a 2000 data set

A. Feinberg, Ph.D., DfRSoft Research, email: dfrsoft@gmail.com

56 In addition, global warming UHI amplification effects have not been quantified to a large degree related to area
57 estimates. Urbanized average solar areas remain unknown.

58
59 In our study, one key paper listed in the Table 1 is due to Schneider et al. (2009) since it is cited by the AR5 2014
60 IPCC report (Satterthwaite et al. 2014). In Schneider's paper, the larger area found in the GRUMP 2005 study
61 (Table 1) is criticized. These area estimates are of interest in our paper for the *Weighted Amplification Albedo Solar*
62 *Urbanization (WAASU) Model*. As well, the Amplification factors we use are related to their urban coverage
63 estimates. In this paper we use both the Schneider et al. and GRUMP studies for the nominal and worst cases
64 urbanization area estimates respectively. Furthermore, they were both done using data sets from around 2000 which
65 is a convenient time to extrapolate down to 1950 and up to 2019 (see Sec. 3).

66
67 In our study, where we introduce the WAASU model, we will see that it has some advantages over the ground-based
68 temperature studies like McKittricks and Michaels. The model is non probabilistic, in line with the way typical
69 energy budgets are calculated. It uses only two key parameters (effective normalized area and average albedo).
70 Because it is simplistic, it has transparency compared with the complex land-based studies.

71 72 *1.1 UHI Amplification Effects*

73
74 The table below lists the global warming causes and amplification effects. In this section we will summarize only
75 the UHI amplification effects listed in the table since the root causes and the main global warming feedback
76 amplification effects are fairly well known.

77
78 **Table 2.** Global warming cause and effects

Global Warming Causes →	Population → Expanding Urban Heat Islands (UHI), Roads & Increases in Greenhouse Gas
Global Warming Feedback Amplification Effects →	Water Vapor Feedback, Land Albedo Change Due to Cities & Roads, Ice and Snow –Albedo Feedback, Lapse Rate Feedback, Cloud Feedback, etc.
Urban Heat Island Amplification Effects →	UHI Solar Heating Area (Building Areas), UHI Building Heat Capacities, Humidity Effects and Hydro-Hotspots, Reduced Wind Cooling, Solar Canyons, Loss of Wetlands, Increase in Impermeable Surfaces, Loss of Evapotranspiration Natural Cooling.

79
80 The UHI amplification effects that we consider to dominate listed in the table are as follows:

- 81
- 82 • ***The humidity amplification effect:*** This has been observed. For example, Zhao et al. (2014) noted that UHI
83 temperature increases in daytime ΔT by 3.0°C in humid climates but decreasing ΔT by 1.5°C in dry
84 climates. They noted that such relationships imply that UHIs will exacerbate heat wave stress on human
85 health in wet UHI climates. One explanation for this is how heat dissipates through convection which is
86 more difficult in humid climates. Another explanation is that warmer air holds more water vapor. This can
87 increase local specific humidity so that there could be local greenhouse effects.
 - 88
 - 89 • ***The heat capacity and solar heating area amplification effect:*** This contributes to the day-night UHI
90 cycle. Here in most cities, it is observed that daytime atmospheric temperatures are actually cooler
91 compared to night. For example, in a study by Basara et al. (2008) in Oklahoma city UHI it was found that
92 at just 9-m height, the UHI was consistently $0.5\text{--}1.75^{\circ}\text{C}$ greater in the urban core than the surrounding rural
93 locations at night. Further, in general UHI impact was strongest during the overnight hours and weakest
94 during the day. This inversion effect can be the results of massive UHI buildings acting like heat sinks,
95 having giant heat capacities and storing heat in their reservoir via convection as solar radiation is absorbed
96 during the day. This often reduces the UHI day effect, but at night buildings cool down, giving off their
97 stored heat that increases local temperatures to the surrounding atmosphere. This effect increases with city
98 growth as buildings have gotten substantially taller (Barr 2019) since 1950.
 - 99
 - 100 • ***The hydro-hotspot amplification effect:*** This effect is not well addressed. Here atmospheric moisture
101 source is a complex issue due to Hydro HotSpots (HHS). Hydro hotspots occur when buildings are hot due
102 to sun exposure. Then during precipitation periods, the hot highly evaporation surfaces increase localized
103 water vapor in the air via the effect that warm air holds more moisture. This increase in local greenhouse
104 gas, could blanket city heat and increase infrared radiation during these periods. This, as discussed above,
105 is another possible UHI humidity amplification.
 - 106
 - 107 • ***Reduced wind cooling and solar canyons:*** In UHIs reduced wind is a known effect due to building wind
108 friction which inhibits cooling by convection. As well, tall buildings create solar canyons and trap sunlight

109 reducing the average albedo although some benefits occurs from shading. In general, both have the effect
 110 of amplifying the temperature profile of UHIs.
 111

112 2 Data and Methods

113
 114 We see from the previous section that estimating climate change impact just based on the UHI and Urban area
 115 coverage as in Table 1, cannot take into account solar heating building sidewall areas, massive heat capacities, the
 116 humidity effects, wind reduction and the solar canyon effect which amplify UHI effects beyond its own climate area.

117 2.1 UHI Area Amplification Factor

118
 119 In order to estimate the UHI amplification effects, it is logical to first look at UHI footprint (FP) studies as they
 120 provide some measurement information. Zhang et al. (2004) found the ecological footprint of urban land cover
 121 extends beyond the perimeter of urban areas, and the footprint of urban climates on vegetation phenology they found
 122 was 2.4 times the size of the actual urban land cover. In a more recent study by Zhou et al. (2015), they looked at
 123 day-night cycles using temperature difference measurements. In this study they found UHI effect decayed
 124 exponentially toward rural areas for majority of the 32 Chinese cities. Their study was very thorough and extended
 125 over the period from 2003 to 2012. They describe China as an ideal area to study since it has experienced the
 126 rapidest urbanization in the world in the decade they evaluated. They found that the “footprint” of UHI effect,
 127 including urban areas, was 2.3 and 3.9 times of urban size for the day and night, respectively. We note that the
 128 average day-night amplification footprint coverage factor is 3.1.

129 Looking at Table 2, we see that the UHI Amplification Factor (AF) is highly complex making it difficult to assess
 130 from first principles as it would be some function of Table 2 components:

$$131 \quad AF_{UHI \text{ for } 2019} = f\left(\overline{Build}_{Area} \times \overline{Build}_{C_p} \times \overline{R}_{wind} \times \overline{LossE}_{vtr} \times \overline{Hy} \times \overline{S}_{canyon}\right) \quad (1)$$

132 were

133 \overline{Build}_{Area} = Average building solar area

134 \overline{Build}_{C_p} = Average building heat capacity

135 \overline{R}_{wind} = Average city wind resistance

136 \overline{LossE}_{vtr} = Average loss of evapotranspiration to natural cooling & loss of wetland

137 \overline{Hy} = Average humidity effect due to hydro-hotspot

138 \overline{S}_{canyon} = Average solar canyon effect

139
 140 As a helpful example, one basic formulation that might be suggested is a product of power law average ratios over
 141 all urban cities compared to a reference year (1950) such that
 142

$$143 \quad AF_{UHI \text{ for } 2019} = \left(\frac{(\overline{Build}_{Area})_{2019}}{(\overline{Build}_{Area})_{1950}}\right)^{N_1} \left(\frac{(\overline{Build}_{C_p})_{2019}}{(\overline{Build}_{C_p})_{1950}}\right)^{N_2} \left(\frac{(\overline{R}_{wind})_{2019}}{(\overline{R}_{wind})_{1950}}\right)^{N_3} \left(\frac{(\overline{LossE}_{vtr})_{2019}}{(\overline{LossE}_{vtr})_{1950}}\right)^{N_4} \left(\frac{(\overline{Hy})_{2019}}{(\overline{Hy})_{1950}}\right)^{N_5} \left(\frac{(\overline{S}_{canyon})_{2019}}{(\overline{S}_{canyon})_{1950}}\right)^{N_6} \cdot (2)$$

144
 145 In order to provide some estimate of this factor, we note that Zhou et al. (2015) found the FP physical area (km²),
 146 correlated tightly and positively with actual urban size having correlation coefficients higher than 79%. This
 147 correlation can be used to provide an initial estimate of this complex factor. Therefore, as a model assumption, it
 148 seems reasonable to use area ratios for this estimate. Area estimates have been obtained in the next Section in Table
 149 3 between 2019 and 1950 time frames. These yield the following results for the Schneider et al. (2009) and the
 150 GRUMP (2005) extrapolated area results:

$$151 \quad AF_{UHI \text{ for } 2019} = \frac{(Urban \text{ Size})_{2019}}{(Urban \text{ Size})_{1950}} \approx \begin{cases} \left(\frac{[0.188]_{2019}}{[0.059]_{1950}}\right)_{Schneider} = 3.19 \\ \left(\frac{[0.952]_{2019}}{[0.316]_{1950}}\right)_{GRUMP} = 3.0 \end{cases} \quad (3)$$

152 Between the two studies, the UHI area amplification factor average is 3.1. Coincidentally, this is the same factor
 153 observed in the Zhou et al. (2015) study for the average footprint. This factor may seem high. However, it is likely
 154 conservative. There are other effects that would be difficult to assess. For example, increases in global draught due
 155 to loss of wet lands, deforestation effects due to urbanization and draught related fires. It could also be important to
 156 factor in changes of other impermeable surfaces since 1950 such as highways, large impermeable surfaces (parking
 157 lots and event centers), and so forth.

158
 159 The area amplification value of 3.1 is then considered as one of our model assumptions.

161 **2.2 Alternate Method Using the UHI's Horizontal Extent**

162
 163 An alternate approach to check the estimate of Equation 3, is to look at the UHI's dome extent. Fan et al. (2017)
 164 using an energy balance model to obtain the maximum horizontal extent of a UHI heat dome in numerous urban
 165 areas found the nighttime extent of 1.5 to 3.5 times the diameter of the city's urban area (2.5 average) and the
 166 daytime value of 2.0 to 3.3 (2.65 average).

167
 168 Applying this energy method (instead of the area ratio factor in Eq. 3), yields a diameter in 2019 compared to that of
 169 1950 increase of about 1.8. This implies a factor of $2.5 \times 1.8 = 4.5$ higher in the night and $2.65 \times 1.8 = 4.8$ in the day in
 170 1950 (average 4.65). This increase occurs 62.5% of the time according to Fan et al., (where their steady state
 171 occurred about 4 hours after sunrise and about 5 hours after sunset) yielding an effective UHI amplification factor of
 172 2.9. We note this amplification factor is in good agreement with Equation 3. Fan et al. assessed the heat flux over the
 173 urban area extent to its neighboring rural area where the air is transported from the urban heat dome flow. Therefore
 174 the heat dome extends in a similar manner as observed in the footprint studies. If we use the dome concept, we can
 175 make an assumption that the actual surface area for the heat flux is increase by the surface area of the dome. We
 176 actually do not know the true diameter of the dome, but it is larger than the assessment by Fan et al.. Using the dome
 177 extend due to Fan et al. applied to the area of diameter D , the amplification factor should be correlated to the ratios
 178 of the dome surface areas as

$$180 \quad AF_{UHI \text{ for } 2019} = \left(\frac{D_{2019}}{D_{1950}} \right)^2 = 2.9^2 = 8.4 \quad (4)$$

181 Thus, this is our second model assumption, where it is reasonable to use the ratios of the dome's surface area for an
 182 alternate approach in estimating the effective UHI amplification factor. In this way we will have two values, 3.1 and
 183 8.4 to work with which will help in assessing model consistency and provide upper and lower bounds for effective
 184 area amplification which must occur based on these authors observations and the dependence in Equation 1.

186 **2.3 Area Extrapolations for 1950 and 2019**

187
 188 In order to assess the urbanized area, (also used in determining the UHI amplification factor ratios above), we need
 189 to project the Schneider and GRUMP area estimates down to 1950 and up to 2019. Both use datasets from around
 190 2000 so this is a convenient somewhat middle time-frame. Here we decided to use the world population growth rate
 191 (World Bank 2018) which varies by year as shown in Appendix A in Figure A1. We used the average growth rate
 192 per $\frac{1}{2}$ decade for iterative projections (about 1.3% to 1.6% per year).

193
 194 To justify this we see that Figure A2a illustrates that building material aggregates (USGS 1900-2006) used to build
 195 cities and roads correlates well to population growth (US Population Growth 1900-2006).

196
 197 It is also interesting to note that building materials for cities and roads also correlates well to global warming trends
 198 (NASA 1900-2006) shown in Figure A2b.

199
 200 Column 2 in Table 3 show the projections with the actual year (~2000) data point tabulated value also listed in the
 201 table (also see Table 1). The UHI area amplification factor of 3.1 (Column 3) are then applied to Schneider and
 202 GRUMP studies shown in Column 4.

203
 204
 205
 206
 207

208

Table 3. Extrapolated and amplified urbanized coverage estimates

Year	Urban coverage percent of Earth	Amplification factor effect	Effective amplification coverage area effect
Schneider study			
1950	0.059*	1	0.059%
2000-2001	0.0051x29%=0.148		
2019	0.188*	3.1 AF _{Area} **	0.583%
2019	0.188*	8.4 AF _{Dome} **	1.58%
Worst case GRUMP study			
1950	0.316%*	1	0.316%
2000	0.027x29%=0.783%		
2019	0.952%*	3.1 AF _{UHI} **	2.95%
2019	0.952%*	8.4 AF _{Dome} **	8%

*Growth rate of cities using world population yearly growth rate in Fig A1, **AF_{UHI} is the area amplification factor for 2019 referenced to 1950.

209
210
211
212

2.4 Weighted Amplification Albedo Solar Urbanization (WAASU) Model Overview

213
214
215

The WAASU model is very straightforward; it is based on a global weighted albedo model. The Earth Albedo is given by

$$Earth\ Albedo = \sum_i \{ \% Effective\ Surface\ Area_i \times Surface\ Item\ Albedo_i \} + Cloud\ Area \times Cloud\ Albedo. \quad (5)$$

216
217
218 Here the effective surface area is given by

$$Effective\ Surface\ Area = Surface\ Area \times \% Solar\ Irradiance. \quad (6)$$

219
220
221
222

We note that the change in the Earth Albedo change over time (from 1950 to 2019), is just a function of the UHI area variation, (when holding all unrelated UHI components fixed), that is

$$\left(\frac{dEA}{dt} \right)_{EA'} = \sum_i \left(Albedo_{UHI} \times Solar\ Irradiance \times \frac{dArea_{UHI}}{dt} \right)_i, \quad (7)$$

223
224
225

where EA is the Earth Albedo, and EA' are all other Earth components (held fixed). Although it is possible that the solar irradiance percent changes due to new city locations, in this model we assume it is fixed at 100%. This indicates, for example, that even if we were to change the *Effective Surface Area* of perhaps the *sea ice component* due to the fact that it receives about 40% irradiance compared with other areas and redistributed its radiance (per the Earth's energy budget), it would not affect the overall results when looking at the albedo change due to the UHI effect from 1950 to 2019. Therefore, the model allows freedom to only work with normalized area coverage changes when focusing on the UHI effect. On the other hand, solar irradiance comes into play for sea ice when we are considering its global albedo effect from 1950 to 2019 (see Appendix C). However, the solar radiation weighting, albedo, and areas for all Earth components are subjected to the constraints below.

226
227

2.4.1 Model Constraints

228
229

This model is subject to the constraint

$$Total\ Area = \sum_i \{ \% Earth\ Surface\ Areas_i \} + \% Cloud\ Area = 100\% \quad (8)$$

230
231

and the normalization constraint for the Earth surface areas (when the UHI area is increased) must then be subject to

232
233

244
$$\sum_i \{ \% Earth Surface Areas_i \} = 100\% - \% Cloud Area. \tag{9}$$

245
 246 To simplify things as much as possible, only five Earth constituents are used: *water, sea ice, land, UHI coverage,*
 247 *and clouds* (where *land* is its area minus the UHI coverage). These components are fairly easy to estimate and
 248 references for their values are provided in Appendix D. Furthermore, we use consistent values found in the IPCC
 249 AR5 report (Hartmann et al., 2013) assessment of the Earth’s energy budget for solar irradiance. Table 4
 250 summarizes the constraints from these IPCC values.

251
 252 The fixed components of our model maintain relative consistency from 1950 to 2019. The non-fixed value is the
 253 urban coverage as indicated by Equation 7. The only unknown value is the *land* albedo (minus the UHI coverage)
 254 and this value is adjusted to obtain the IPCC global albedo of 29.4118% and its *land* value of incident/reflected
 255 value of 7.0588.

256 **Table 4.** IPCC Earth energy budget values (Hartmann et al., 2013)

IPCC Item	Incident and Reflected Radiation (W/m ²)	Albedo %	Absorbed (W/m ²)
Earth	100/340	29.4118	240=340x(1-.294)
Atmosphere & Clouds	76/340	22.3529	79
Earth Surface Albedo	24/340	7.0588	161

257
 258
 259 These values are used as a 1950 starting point and then the 2019 increase for UHI coverage area is inserted. This
 260 increases the Earth’s area to greater than 100%. Therefore, renormalization is done per the constraint of Equation 9
 261 (detailed in Appendix B).

262
 263 **3 Results and discussion**

264
 265 Using the extrapolated area coverage in Table 3 with the 3.1 amplification factor applied to the urbanized growth,
 266 the resulting global albedo change occurred of 29.3956% in 2019 (Table 5b) compared to the earlier 1950 albedo
 267 value of 29.4118% (Table 5a) for the Schneider nominal case. As well, for the GRUMP worst case, the albedo
 268 changed from 29.4118% (Table 6a) to 29.3322% (Table 6b) due to the urbanized growth.

269
 270 As we mentioned earlier, the increases in the solar surface area of the Earth, which will occur with city growth of
 271 tall buildings and their solar areas, however comparatively small, requires renormalization in the model of the Earth
 272 surface components of the WAASU model (detailed in Appendix B). This is displayed in column 3 in Tables 5b and
 273 6b. While the model is sensitive to urban coverage changes, it works well with renormalization showing a high level
 274 of consistency to urban coverage proportionality changes. This is indicated in Table 7 where we find the GRUMP
 275 2019 area feedback is 0.0944% (W/m²)/Norm Area (=0.271/2.87) compared with the Schneider area feedback of
 276 0.0948 (W/m²)/ %Norm Area (=0.055/0.58).

277
 278 **Table 5a.** Schneider results (Albedo=29.4118, 1950) **Table 5b.** Schneider results (Albedo=29.3956%, 2019)

Surface	Albedo	% Area of Surface	Normalized Earth Area	Weighted Albedo %
	A	B	C=A x B x (1-0.67)	A x C
Sum of Water Type		71		
Sea Ice	0.6	15	4.95	2.970
Water	0.06	56	18.48	1.109
Sum of Land Type		29		
Land - (UHI + Coverage)	0.3118	28.941	9.55053	2.978
UHI + Coverage	0.12	0.059	0.01947	0.002
		Σ=100.000	33.000	7.05882
			Cloud Area	
Clouds	0.3336	67	67	22.35294
Σ Sum Earth %			100.000	
Σ Global Albedo				29.4118

Surface	Albedo	Normalized % Surface Area	Normalized Earth Area	Weighted Albedo %
	A	B	C=A x B x (1-0.67)	A x C
Sum of Water Type		70.6298		
Sea Ice	0.6	14.9218	4.924194	2.955
Water	0.06	55.7081	18.383673	1.103
Sum of Land Type		29.37		
Land - (UHI + Coverage)	0.3118	28.79	9.5007	2.962
UHI + Coverage	0.12	0.58	0.1914	0.023
		Σ=100.000	33.000	7.0197
			Cloud Area	
Clouds	0.3336	67	67	22.3529
Σ Sum Earth %			100.000	
Σ Global Albedo				29.3956

279
 280

281 **Table 6a.** GRUMP results (Albedo=29.4118, 1950) **Table 6b.** GRUMP results (Albedo=29.3322%, 2019)

Surface	Albedo		Normalized	Weighted	Surface	Albedo		Normalized	Normalized	Weighted
	A	B	% Surface Area	Earth Area Albedo %		A	B	% Surface Area	Earth Area Albedo %	
			C=A x B x (1-0.67)	A x C				C=A x B x (1-0.67)	A x C	
Sum of Water Type		71			Sum of Water Type		69.1778			
Sea Ice	0.6	15	4.95	2.970	Sea Ice	0.6	14.615	4.82295	2.894	
Water	0.06	56	18.48	1.109	Water	0.06	54.5628	18.005724	1.080	
Sum of Land Type		29			Sum of Land Type		30.8221			
Land - (UHI + Coverage)	0.3135	28.684	9.46572	2.968	Land - (UHI + Coverage)	0.3135	27.9478	9.222774	2.891	
UHI + Coverage	0.12	0.316	0.10428	0.013	UHI + Coverage	0.12	2.8743	0.948519	0.114	
Sum Surface %		Σ=100.000	33.000	7.0588	Sum Earth %		Σ=100.000	33.000	6.8655	
			Cloud Area					Cloud Area		
Clouds	0.3336	67	67	22.3529	Clouds	0.3336	67	67	22.3529	
Σ Sum Earth %			100.000		Σ Sum Earth %			100.000		
Σ Global Albedo				29.4118	Σ Global Albedo				29.3322	

282
 283 Table 7 provides a summary of albedo changes found in the WASSU model along with the expected solar long wave
 284 radiation increase. From the above global WAASU model, the estimates of the Earth’s radiated long wavelength
 285 emissions are set equal to the short wave radiation absorption:

286
 287
$$P_{Total} = 340 \text{ W/m}^2 (1 - \text{Albedo}). \tag{10}$$

288
 289 Then the change from 1950 to 2019 represents the equivalent increase in long wave radiation is given by

290
 291
$$\Delta P_{Total} = 340 \text{ W/m}^2 \{ (1 - \text{Albedo})_{2019} - (1 - \text{Albedo})_{1950} \}. \tag{11}$$

292
 293 Results are compiled in Table 7. The table also includes “what if” estimates, if we could change urbanization to be
 294 more reflective with cool roofs to reverse the effect.

295
 296 **Table 7.** Albedo and radiative increase model results with UHI effective area.

297

Year	Urban Extent Global Area %	UHI Effective Global Surface % Area	Normalized UHI Effective Global Surface %Area	Albedo Cities	Global Weighted Albedo	ΔP _{Total} UHI Radiative Increase W/m ² (%GW)*	Model Feedback
							$\frac{\Delta P_{Total} (W/m^2)}{Norm\% Area / ^\circ K}$ $\left(\frac{\Delta P_{Total} (W/m^2)}{Norm\% Area} \right)$
Nominal Case Schneider Study							
1950	0.059	0.059	0.059	0.12	29.4118	0	—
2019	.188	0.583 (Area AF)	0.58	0.12	29.3956	0.055 (1.54%)*	0.10 (0.094)
2019	.188	1.58 (Dome AF)	1.56	0.12	29.3654	0.158 (4.41%)*	0.106 (0.101)
What if	0.188	0.583, 1.58 (Area-Dome AF)	0.58, 1.56	0.204, 0.210	29.4118	-0.055-0.158 (-1.54, -4.41%)*	—
Worst Case GRUMP Study							
1950	0.316%	0.316	0.316	0.12	29.4118	0	—
2019	0.952%	2.95 (Area AF)	2.8743	0.12	29.3322	0.271 (7.6%)*	0.099 (0.94)
2019	0.952%	8.0 (Dome AF)	7.429	0.12	29.1907	0.752 (21%)*	0.107 (0.101)
What if	0.952%	2.95	2.8743	0.2039, 0.21	29.4118	-0.271 (-7.6%)*	—

298 *Percent of Warming estimate, $P = 340 \times (1 - \text{Albedo})$, $\%GW = \{ (P/\epsilon\sigma)_{2019}^{0.25} - (P/\epsilon\sigma)_{1950}^{0.25} \} / 0.95^\circ\text{C}$, $\epsilon = 1$

299
 300 The general results are summarized:

- 301
 302 • Nominal Schneider case from 1950 to 2019 is 0.055 and 0.158 W/m² due to urban area and dome
 303 amplification coverage respectively. These would equate to about 1.55% and 4.4% of global warming
 assuming the total increase from 1950 is about 0.95°C in 2019.

- 304 • Worst GRUMP case from 1950 to 2019 is 0.271 and 0.752 W/m² due to urban area and dome amplification
 305 coverage respectively. This would roughly equate to about 7.5 and 21% of global warming assuming the
 306 total increase from 1950 is about 0.95°C in 2019.
 307 • We note the consistency of the feedback parameter having quite small variability and averaging about
 308 0.102 W/m²/Normalized Area/°K.
 309 • “What if” corrective action results of cool roofs indicates that changing city albedos in both the Schneider
 310 and the GRUMP case from 0.12 to an average value of 0.207 would reverse the increase in emission back
 311 to 1950 levels.
 312

313 Model consistency is indicated in the area feedback column in Table 7. Furthermore, we note that radiation increase
 314 goes as the area changes. For example, the Schneider to Grump normalized area increase from 0.58 (Schneider) to
 315 2.8743% (GRUMP) yields a factor of 3.96 $(= (2.874 - .58) / .58)$. This can be compared to the observed long radiation
 316 increase from 0.055 W/M2 (Schneider) to 0.271 W/M2 (GRUMP) that also yields a similar factor of 3.93 $(= (0.271 -$
 317 $.055) / .055)$. This observation along with the feedback values can be helpful in estimating future warming trends due
 318 to UHI growth rates, which at the present time from Figure A1, is about 1.2% per year. We also note that in both the
 319 Schneider and GRUMP case, implementing cool roof requires about the same albedo change from 0.12 to 0.207 in
 320 order to reverse the warming trend.
 321

322 Although global warming assessment obtained in the WAASU model, especially for the Schneider case does not
 323 appear to show much contribution to global warming, we find that climate feedback estimates increase the estimated
 324 root-cause proportion significantly. Examples are provide in Appendix C that help to demonstrate how the root-
 325 cause global warming contribution can be as go as high as 11% for the Schneider case and 38% for the GRUMP
 326 case (see Table C2).
 327

328 4 Conclusions

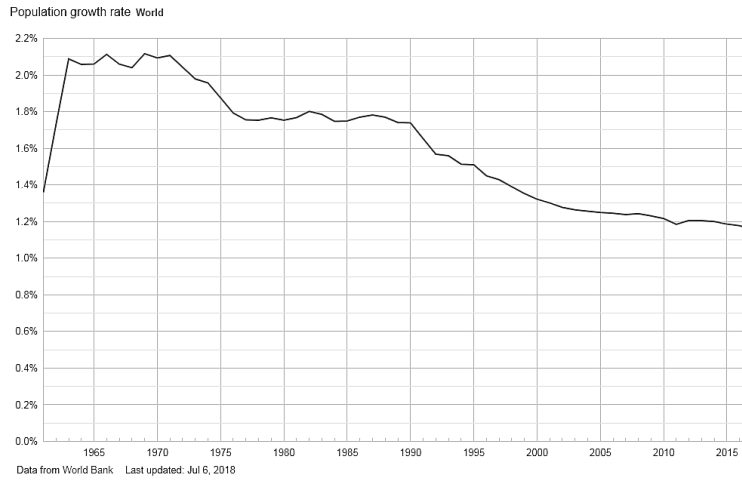
329
 330 In this paper we were able to provide estimates of UHI effect (with urban area) on global warming. This was done
 331 with the aid of assumptions for area UHI amplification factors. These estimates inserted into our WAASU model
 332 found that between 0.055 and 0.752 W/m² of radiative forcing is possible according the WAASU model (this results
 333 indicates that about 1.6 and 21% of global warming may be due to the UHI effect (with urban areas). This wide
 334 variation is due to both the amplification and urban area uncertainties. However, the model found that the effective
 335 UHI feedback estimates were consistent and about 0.1 (W/m²)/°K/%Normalized Area. Examples are provided in
 336 Appendix C to illustrate how the UHI root-cause assessment to global warming increases significantly when all
 337 climate feedback factor contributions are considered. The strength of the model is also demonstrated in Appendix C
 338 as estimates were obtained for global warming to the loss of sea ice in the last two decades. As area estimates and
 339 UHI amplification factors are very sensitive to the final results, it is clear refined values of both would be important
 340 for further study.
 341

342 Below we provide suggestions and corrective actions which include:

- 343 • IPCC be more proactive in helping to providing albedo guidelines or recommendation similar to their CO₂
 344 effort for both UHIs and roads.
 345 • A guideline for future albedo design requirements of city and roads should be developed.
 346 • Recommend an agency like NASA be tasked with finding applicable solutions to cool down UHIs.
 347 • Recommendation for cars to be more reflective. Here although world-wide cars likely do not embody much
 348 of the Earth’s area, recommending that all new manufactured cars be higher in reflectivity (e.g., silver or
 349 white) would help raise awareness of this issue similar to electric cars that help improve CO₂ emissions.
 350

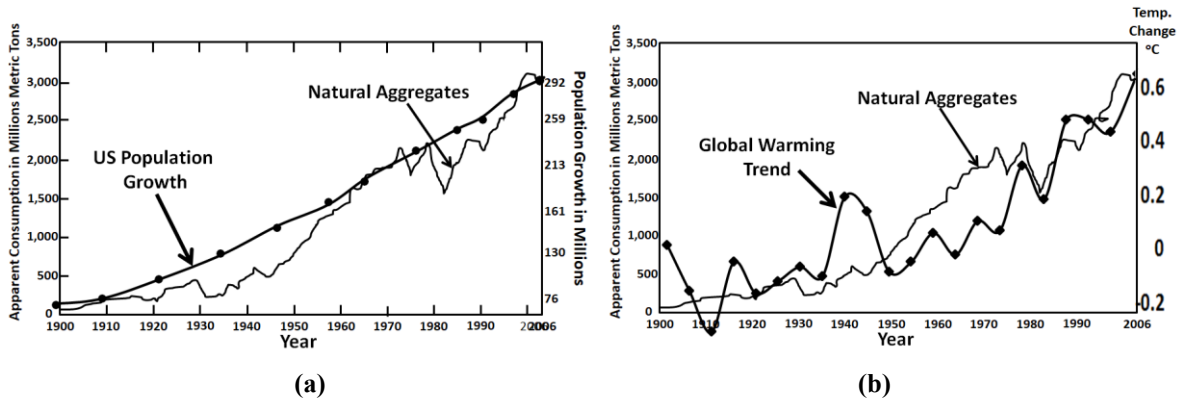
351 Appendix A: Growth Rates and Information on Natural Aggregates

352
 353 Below is a plot of the world population growth rate that varies from about 2.1 to 1.1. This is used to make growth
 354 rate estimates of urban coverage. We note that natural aggregate used to build cities and roads are reasonably
 355 correlated to population growth in Figure A2a. Also of interest (Fig. A2b) is the fact that one can see some
 356 correlation to global warming with the use of natural aggregates.



357
358

Figure A1. Population growth rate by year from 1960 to 2018, World Bank, 2018



359
360

Figure A2. a) Natural aggregates correlated to U.S. Population Growth (USGS 1900-2006) b) Natural aggregates correlated to global warming (NASA 2020)

362
363

Appendix B: Albedo Model Normalization Information

364
365

Table 5a is reproduced from above, while Table 5b is the results of the Schneider dome area case. The results is used to demonstrate how normalization is performed

366
367
368
369

Table 5a. Schneider results (Albedo=29.4118, 1950) Table 5b. Schneider results (Albedo=29.3654%, 2019)

Surface	Albedo	% Area of Surface	Normalized Weighted Earth Area	Normalized Weighted Albedo %
	A	B	$C=A \times B \times (1-0.67)$	$A \times C$
Sum of Water Type		71		
Sea Ice	0.6	15	4.95	2.970
Water	0.06	56	18.48	1.109
Sum of Land Type		29		
Land - (UHI + Coverage)	0.3118	28.941	9.55053	2.978
UHI + Coverage	0.12	0.059	0.01947	0.002
		$\Sigma=100.000$	33.000	7.05882
			Cloud Area	
Clouds	0.3336	67	67	22.35294
Σ Sum Earth %			100.000	
Σ Global Albedo				29.4118

Surface	Albedo	Normalized % Surface Area	Normalized Weighted Earth Area	Normalized Weighted Albedo %
	A	B	$C=A \times B \times (1-0.67)$	$A \times C$
Sum of Water Type		69.93626		
Sea Ice	0.6	14.77526	4.8758358	2.955
Water	0.06	55.161	18.20313	1.092
Sum of Land Type		30.064		
Land - (UHI + Coverage)	0.3118	28.5074	9.407442	2.933
UHI + Coverage	0.12	1.5563	0.513579	0.062
		$\Sigma=100.000$	33.000	6.9507
			Cloud Area	
Clouds	0.3336	67	67	22.3530
Σ Sum Earth %			100.000	
Σ Global Albedo				29.3654

370
371

Normalization is done as follows:

372
373
374
375
376
377

1. Model starts with 1950 Table 5a albedo 29.4118%, then 2019 urban coverage area is entered.
2. For example, in Table B1, the new area increases from 0.059% to .158%. This is 1.521% larger, now the 'Sum of % of Earth Area' will be 101.521% in 2019.
3. All areas are renormalized to 101.521%. For example, sea ice at 15% in 1950 becomes $15\% \times (100.000/101.521) = 14.775\%$ and the Urban Coverage becomes $1.58\% \times (100/101.521) = 1.556\%$.

378 Appendix C: Related Warming Estimates and Other Amplification Factors

379

380 Although the results obtained here at first seem to indicate that UHIs do not appear to contribute much to global
 381 warming, when other factors are considered, much stronger significance can be estimated. In this appendix,
 382 additional feedback factors are suggested providing a number of global warming estimates.

383

- 384 • *Such factors can be contentious; however, it is not uncommon to look at how factors effect each other*
 385 *climate science. Therefore, we have chosen to provide these in this appendix mainly as an aid for the*
 386 *reader to illustrate how climate sensitivity can factor into the magnitude of UHIs warming significance.*
 387 *These estimates should be considered only as ballpark values.*

388

389 C.1 Global Feedback Amplification Factors

390

391 There is a wide range of possible estimates of climate feedback sensitivity driven by uncertainties in how water
 392 vapor, clouds, and other factors change as the Earth warms. Climate feedbacks are mixed and some will amplify
 393 (positive feedback) or diminish the effect of warming from the root cause effects (see for example Hausfather 2018).
 394 The actual feedback is known to be positive (van Nes, 2015). Climatologists will often approximate such factors
 395 frequently in reference with CO₂ doubling theory as positive. For example, water-vapor feedback alone, which is
 396 one of the most important in our climate system, is thought to have the capacity to about double the direct warming
 397 (Manabe and Wetherald, 1967; Randall et al., 2007, Dessler et. Al, 2008). This results from the fact that warm air
 398 holds more greenhouse moisture gas. Climate models incorporate this feedback. Water vapor feedback is strongly
 399 positive, with most evidence supporting a magnitude of 1.6 to 2.0 W/m²/K (Dessler et. al., 2008). Also water vapor
 400 feedback is considered a faster feedback mechanism (Hansen, 2008). We will use a factor of 1.75, a bit less than a
 401 doubling factor of 2. This factor would apply equally to UHI warming contribution, Greenhouse Gases (GHG), or
 402 warming due to sea ice melting.

403

404 C.2 WAASU Model Applied to the Melting of Sea Ice

405

406 While the Antarctic sea ice has remained roughly constant, the Arctic sea ice is melting at an alarming rate of
 407 12.85% in the last two decades (NASA sea ice, 2019). This apparent trend appears to yield about a 26% change in
 408 sea ice loss. It is difficult to find a strong reference for quantifying global warming impact due to Arctic sea ice
 409 melting. However, we might get a rough ballpark approximation using the WAASU model (and also illustrate one of
 410 the strengths of the model). Sea ice melting will results in a significant albedo change that roughly change in ice
 411 albedo of 0.6, to the open ocean albedo of 0.06 (see Table C1 and C2). Fortunately, the Arctic areas receive only
 412 about 40% as much solar radiation (Sciencing, 2018) reducing the feedback effect. From Equation 6, the effective
 413 sea ice surface area reduction from the irradiance decrease can be approximated as

414

$$415 \text{ Effective sea ice surface area} = 15\% (1 - 0.26 \times 0.40) = 13.44\% \text{ (a 1.56\% reduction of effective area).} \quad (\text{C-1})$$

416

417 In the WAASU model, we will have to make an assumption that the effective ocean surface area increases
 418 proportionately by 1.56% to 57.56% (see Table C2). The model then finds that the global albedo change decreases
 419 from 29.4118 to 28.9948%. (Note that alternately we could have set the albedo to 29.4118% in 2019 and worked
 420 back to 1950. In this case the albedo would have increase to 29.83%).

421

422 The Global Warming (GW) is found as:

$$423 \%GW = \{(P/\epsilon\sigma)^{0.25}_{2019} - (P/\epsilon\sigma)^{0.25}_{1950}\} / 0.95^\circ\text{C}, \quad (\text{C-2})$$

424

425 where $P = 340 \text{ W/m}^2 \times (1 - \text{Albedo})$ and $\epsilon = 1$. The warming increase due to ice melting is estimated from this model to
 426 be about 0.25°C or 26.4% of the 0.95°C increase in 2019. The increase in radiative forcing is 0.9452 W/m². The
 427 feedback is then roughly 1 W/m²/K where we assume a temperature change of 0.95C over this time period.

428

429 This estimate should only be taken as ballpark due to numerous uncertainties as climatologists find it hard to fully
 430 quantify the seasonal variations in ice change and to know the possible impact on cloud coverage increase from
 431 additional warming evaporation. However, one would expect less evaporation in the Arctic. Thus, there are a lot of
 432 uncertainties.

433 **Table C1.** Schneider results (Albedo=29.4118, 1950) **Table C2.** Sea ice loss - albedo change (29.0643%, 2019)

Surface	Albedo	% Area of Surface	Normalized Earth Area	Weighted Albedo %
	A	B	C=A x B x (1-0.67)	A x C
Sum of Water Type		71		
Sea Ice	0.6	15	4.95	2.970
Water	0.06	56	18.48	1.109
155Sum of Land Type		29		
Land - (UHI + Coverage)	0.3118	28.941	9.55053	2.978
UHI + Coverage	0.12	0.059	0.01947	0.002
		Σ=100.000	33.000	7.05882
			Cloud Area	
Clouds	0.3336	67	67	22.35294
Σ Sum Earth %			100.000	
Σ Global Albedo				29.4118

Surface	Albedo	Normalized % Surface Area	Normalized Earth Area	Weighted Albedo %
	A	B	C=A x B x (1-0.67)	A x C
Sum of Water Type		71		
Sea Ice	0.6	13.44	4.4352	2.507
Water	0.06	57.56	18.9948	1.14
Sum of Land Type		29	23.43	
Land - (UHI + Coverage)	0.3118	28.941	9.55053	2.978
UHI + Coverage	0.12	0.059	0.01947	0.002
		100.000	33.000	6.6395
			Cloud Area	
Clouds	0.3336	67	67	22.3530
Σ Sum Earth %			123.430	
Σ Global Albedo				29.1338

434
435 **C.3 Ballpark Contributions to Global Warming**

436
437 Table C3 summarizes the key global warming cause and effect factors that we have described.

438
439 **Table C3.** Global warming factors of interest

Urban Climate Amplification	Effects	Where Applied
UHI Area Amplification Factor	3.1 UHI Amplification	Applied to 2019 UHI Area
UHI Dome Horizontal Method	2.9 UHI Amplification	Applied to 2019 UHI Area
Ice Melting	0.25°C	25°C out of 0.95°C
Atmospheric Moisture Increase	1.75 GW Amplification	Applied to Ice Melting Temp, UHI, and GHGs +X*

440 where X is any other feedbacks (positive or negative)

441
442 Then major contributions to global warming can be simplified as follows for steady state warming

443
444
$$\Delta T_{GW} = \Delta T_{UHI} + \Delta T_{Water-Vapor} + \Delta T_{Sea-Ice} + \Delta T_{GHG} + \Delta T_X, \tag{C-3}$$

445
446 where $\Delta T_{GW}=0.95^\circ\text{C}$, $\Delta T_{UHI-Schneider}=0.0147^\circ\text{C}$ (Table 7), $\Delta T_{Sea-Ice}=0.25^\circ\text{C}$, λ is the feedback, and ΔF is the radiative forcing change. We have two unknowns $\Delta T_{Water-Vapor}$ and ΔT_{GHG+X} . Here X is for all other feedback mechanisms like lapse rate and increases in cloud coverage, so it can be both both positive or negative. These unknowns may be

447
448
449
450
451
$$0.95^\circ\text{C} = AF_{water\ vapor}(\Delta T_{UHI} + \Delta T_{GHG}) + \Delta T_X + \Delta T_{Sea-Ice} = 1.75(0.0146^\circ\text{C} + \Delta T_{GHG}) + \Delta T_X + 0.25^\circ\text{C} \tag{C-4}$$

452 and
453
$$0.95^\circ\text{C} = \Delta T_{UHI} + \Delta T_{GHG+X} + \Delta T_{Sea-Ice} + \Delta T_{Water-Vapor} = 0.0147^\circ\text{C} + \Delta T_{GHG+X} + 0.25^\circ\text{C} + \Delta T_{Water-Vapor}. \tag{C-5}$$

454
455 With three unknowns and only two equations, at this point we need to make an assumption. We will assume that
456 $T_{GHG}=35\%$ of global warming, or $T_{GHG}=0.3325^\circ\text{C}$. We note that there has been about a 33% increase in CO₂ since
457 1950. Therefore, this is just a rough possible estimate we can provide some examples, yet if this value is known,
458 one can apply it as illustrated here. Using this estimate, with the water vapor $AF_{water-vapor}=1.75$ discussed above, and
459 equation C-4 and C5, we obtain the examples in Table C3.

460
461 We note that in terms of root-causes, these examples illustrate how it is possible for the UHI effect (and coverage)
462 contribution to global warming could range between 4.2 to 38%.

463
464 From the table the UHI effective feedback contribution are 2.73 (4.2%/1.54%), 2.54 (11.2%/4.41%), 2.34
465 (17.8%/7.7%) , 1.79 (37.5%/21%) averaging 2.35. This indicates that the UHI area feedback contribution could
466 increase by 2.35 from 0.1 to about 0.24 W/m²/%Normalized Area (see Table 7). Although these values are crude
467 estimates, they serve as possible helpful examples.

469

Table C3. Global warming contributions (2019)

Warming Component	Temperature Contribution (°C)	% of GW Root Cause	Percent of GW	Temperature Contribution (°C)	% of GW Root Cause	Percent of GW
Schneider Study						
	UHI Area Amplification=3.1			UHI Dome Amplification=8.4		
Urbanization	0.0146	4.2	1.54	0.0419	11.2%	4.41%
Greenhouse gases (35%)	0.3325	95.8	35	0.333	88.8%	35.0%
Sea ice melting feedback	0.25		26.32	0.25		26.32%
Water vapor feedback	.262		27.6	0.285		29.96%
X (Other)	0.091		9.6	0.041		4.31%
Total	∑0.95					
GRUMP Study						
	UHI Area Amplification=3.1			UHI Dome Amplification=8.4		
Urbanization	0.0722	17.8%	7.60%	0.20	37.5%	21.0%
Greenhouse gases (35%)	0.3325	82.2%	35.00%	0.33	62.5%	35.0%
Sea ice melting feedback	0.25		26.32%	0.25		26.3%
Water vapor feedback	0.310175		32.65%	0.417		43.9%
X (Other)	-0.014875		-1.57%	-0.249		-26.3%
Total	∑0.95					

470

471 **Appendix D: WAASU Model References**

472

473 Table D1 provides references for the WAASU model values.

474

475

Table D1 Key References for WAASU model

Parameter	Albedo (reference)	1950 Area (reference)
Sea Ice	50-70%, average 60% (NSID 2020)	15% (Lindsey 2019)
Water	0.06 (NSIDC 2020)	56% Ocean+Sea Ice=71% (USGS)
Land-(UHI+Coverage)	Adjusted to obtain 29.412% and surface reflected of 7.06 Earth Albedo in 1950 thereafter held fixed (see IPCC Hartmann (2013) AR5 report)	29%-Urban Coverage
UHI+Cov	0.12 Sugawara et. Al (2014)	See Table 1
Clouds	22.35294 (IPCC Hartmann et al., 2013)	67% (Earthobservatory, NASA)
Earth Albedo	29.412% (IPCC Hartmann, 2013)	-

476

477

478 **References**

479

480 Barr J. M., 2019 The Economics of Skyscraper Height (Part IV): Construction Costs Around the World,

481 <https://buildingtheskyline.org/skyscraper-height-iv/>

482 Basara J. ,P. Hall Jr. , A.Schroeder , B.Illston ,K.Nemunaitis 2008, Diurnal cycle of the Oklahoma City urban heat island, J. of Geophysical Research

483 Cao C.X. , Zhao J., P. Gong, G. R. MA, D.M. Bao, K.Tian, Wetland changes and droughts in southwestern China, Geomatics, Natural Hazards and Risk, Oct 2011,

484 <https://www.tandfonline.com/doi/full/10.1080/19475705.2011.588253>485 Cormack L. 2015 Where does all the stormwater go after the Sydney weather clears? The Sydney Morning Herald, <https://www.smh.com.au/environment/where-does-all-the-stormwater-go-after-the-sydney-weather-clears-20150430-1mx4ep.html>486 Dessler A. E. ,Zhang Z., Yang P., Water-vapor climate feedback inferred from climate fluctuations, 2003–2008, *Geophysical Research Letters*, (2008), <https://doi.org/10.1029/2008GL035333>487 Earthobservatory, NASA (clouds albedo 0.67) <https://earthobservatory.nasa.gov/images/85843/cloudy-earth>488 Fan, Y., Li, Y., Bejan, A. *et al.* Horizontal extent of the urban heat dome flow. *Sci Rep* 7, 11681 (2017). <https://doi.org/10.1038/s41598-017-09917-4>489 Feddema, J. J., K. W. Oleson, G. B. Bonan, L. O. Mearns, L. E. Buja, G. A. Meehl, and W. M. Washington (2005), The importance of land-cover change in simulating future climates, *Science*, **310**, 1674– 1678, doi:10.1126/science.1118160490 Galka M. 2016, Half the World Lives on 1% of Its Land, Mapped, <https://www.citylab.com/equity/2016/01/half-earth-world-population-land-map/422748/>, (2016 publication on 2000 data set, <http://metrocosm.com/world-population-split-in-half-map/>

500

- 501 Global Rural Urban Mapping Project (GRUMP) 2005, Columbia University Socioeconomic Data and Applications
 502 Center, Gridded Population of the World and the Global Rural-Urban Mapping Project (GRUMP).
- 503 Hansen, J., "2008: Tipping point: Perspective of a climatologist." Archived 2011-10-22 at the Wayback Machine,
 504 Wildlife Conservation Society/Island Press, 2008. Retrieved 2010.
- 505 Hartmann, D.L., A.M.G. Klein Tank, M. Rusticucci, L.V. Alexander, S. Brönnimann, Y. Charabi, F.J. Dentener,
 506 E.J. Dlugokencky, D.R. Easterling, A. Kaplan, B.J. Soden, P.W. Thorne, M. Wild and P.M. Zhai, 2013:
 507 Observations: Atmosphere and Surface. In: Climate Change 2013: The Physical Science Basis. Contribution of
 508 Working Group I to the Fifth Assessment Report of the Intergovernmental Panel on Climate Change [Stocker,
 509 T.F., D. Qin, G.-K. Plattner, M. Tignor, S.K. Allen, J. Boschung, A. Nauels, Y. Xia, V. Bex and P.M. Midgley
 510 (eds.)]. Cambridge University Press, Cambridge, United Kingdom and New York, NY, USA.
- 511 Hirshi M. ,Seneviratne S. , V. Alexandrov, F. Boberg, C. Boroneant, O. Christensen, H. Formayer, B. Orlowsky &
 512 P. Stepanek, Observational evidence for soil-moisture impact on hot extremes in Europe, *Nature Geoscience* 4,
 513 17-21 (2011)
- 514 Huang Q. , Lu Y. 2015 Effect of Urban Heat Island on Climate Warming in the Yangtze River Delta Urban
 515 Agglomeration in China, *Intern. J. of Environmental Research and Public Health* 12 (8): 8773 (30%)
- 516 Jones, P. D., D. H. Lister, and Q.-X. Li, 2008: Urbanization effects in large-scale temperature records, with an
 517 emphasis on China. *J. Geophys. Res.*, 113, D16122, doi: 10.1029/2008JD009916.
- 518 Lindsey R, Scott M., (2019), Climate Change: Arctic Sea Ice Summer Minimum, NOAA Climate.gov,
 519 <https://www.climate.gov/news-features/understanding-climate/climate-change-minimum-arctic-sea-ice-extent>
- 520 Manabe, S., and R. T. Wetherald (1967), Thermal equilibrium of atmosphere with a given distribution of relative
 521 humidity, *J. Atmos. Sci.*, 24, 241–259.
- 522 McKittrick R. and Michaels J. 2004. A Test of Corrections for Extraneous Signals in Gridded Surface Temperature
 523 Data, *Climate Research*
- 524 McKittrick R., Michaels P. 2007 Quantifying the influence of anthropogenic surface processes and inhomogeneities
 525 on gridded global climate data, *J. of Geophysical Research-Atmospheres*
- 526 McKittrick Website Describing controversy: <https://www.rossmckittrick.com/temperature-data-quality.html>
 527 NASA 1900-2006 updated, 2020 <https://climate.nasa.gov/vital-signs/global-temperature/>
- 528 NASA 2000, Gridded population of the world, , [https://sedac.ciesin.columbia.edu/data/set/gpw-v3-population-](https://sedac.ciesin.columbia.edu/data/set/gpw-v3-population-count/data-download)
 529 [count/data-download](https://sedac.ciesin.columbia.edu/data/set/gpw-v3-population-count/data-download)
- 530 NASA Sea Ice, (2019) <https://climate.nasa.gov/vital-signs/arctic-sea-ice/>
- 531 NSID 2020, National Snow & Ice Data Center, "Thermodynamics: Albedo". nsidc.org. Retrieved 14 August 2016.
 532 <https://nsidc.org/cryosphere/seaice/processes/albedo.html>
- 533 Randall, D. A. et al. (2007), Climate models and their evaluation, in *Climate Change 2007: The Physical Science*
 534 *Basis. Contributions of Working Group I to the Fourth Assessment Report of the Intergovernmental Panel on*
 535 *Climate Change*, edited by S. Solomon et al., pp. 591–662, Cambridge Univ. Press, Cambridge, U.K.
- 536 Ren, G.; Chu, Z.; Chen, Z.; Ren, Y. 2007 Implications of temporal change in urban heat island intensity observed at
 537 Beijing and Wuhan stations. *Geophys. Res. Lett.* , 34, L05711,doi:10.1029/2006GL027927.
- 538 Ren, G.-Y., Z.-Y. Chu, J.-X. Zhou, et al., (2008): Urbanization effects on observed surface air temperature in North
 539 China. *J. Climate*, 21, 1333-1348
- 540 Schmidt G. A. 2009 Spurious correlations between recent warming and indices of local economic activity, *Int. J. of*
 541 *Climatology*
- 542 Schneider, A., M. Friedl, and D. Potere, 2009: A new map of global urban extent from MODIS satellite data.
 543 *Environmental Research Letters*, 4(4), 044003, doi:10.1088/1748-9326/4/4/044003
- 544 Satterthwaite D.E., F. Aragón-Durand, J. Corfee-Morlot, R.B.R. Kiunsi, M. Pelling, D.C. Roberts, and W. Solecki,
 545 2014: Urban areas. In: *Climate Change 2014: Impacts, Adaptation, and Vulnerability. Part A: Global and*
 546 *Sectoral Aspects. Contribution of Working Group II to the Fifth Assessment Report of the Intergovernmental*
 547 *Panel on Climate Change (IPCC)*
- 548 Sciencing (2018) <https://sciencing.com/sun-intensity-vs-angle-23529.html>
- 549 Stone B. 2009 Land use as climate change mitigation, *Environ. Sci. Technol.*, 43(24), 9052– 9056,
 550 doi:10.1021/es902150g
- 551 Sugawara, H., Takamura, T. Surface Albedo in Cities (0.12): Case Study in Sapporo and Tokyo, Japan. *Boundary-*
 552 *Layer Meteorol* 153, 539–553 (2014). <https://doi.org/10.1007/s10546-014-9952-0>
- 553 US Population Growth 1900-2006, u-s-history.com/pages/h980.html
- 554 USGS 1900-2006, Materials in Use in U.S. Interstate Highways, <https://pubs.usgs.gov/fs/2006/3127/2006-3127.pdf>
- 555 USGS on Amount of Earth covered by water, [https://www.usgs.gov/special-topic/water-science-](https://www.usgs.gov/special-topic/water-science-school/science/how-much-water-there-earth?qt-science_center_objects=0#qt-science_center_objects)
 556 [school/science/how-much-water-there-earth?qt-science_center_objects=0#qt-science_center_objects](https://www.usgs.gov/special-topic/water-science-school/science/how-much-water-there-earth?qt-science_center_objects=0#qt-science_center_objects)
- 557 van Nes E. H., Scheffer M., Brovkin V., Lenton T. M., Ye H, Deyle E. and Sugihara G., *Nature Climate Change*
 558 2015. [dx.doi.org/10.1038/nclimate2568](https://doi.org/10.1038/nclimate2568)
- 559 World Bank, 2018 population growth rate, worldbank.org
- 560 Yang, X.; Hou, Y.; Chen, B. 2011 Observed surface warming induced by urbanization in east China. *J. Geophys.*
 561 *Res. Atmos*, 116, doi:10.1029/2010JD015452.

- 562 Zhang, X., Friedl, M. A., Schaaf, C. B., Strahler, A. H. & Schneider, A. 2004 The footprint of urban climates on
563 vegetation phenology. *Geophys. Res. Lett.* 31, L12209
- 564 Zhao, Z.-C., 1991: Temperature change in China for the last 39 years and urban effects. *Meteorological Monthly* (in
565 Chinese), 17(4), 14-17.
- 566 Zhao, Z.-C., 2011: Impacts of urbanization on climate change. in: 10,000 Scientific Difficult Problems: Earth
567 Science, 10,000 scientific difficult problems Earth Science Committee Eds., Science Press, 843-846. 30%
- 568 Zhao L, Lee X, Smith RB, Oleson K, Strong 2014, contributions of local background climate to urban heat islands,
569 *Nature*. 10;511(7508):216-9. doi: 10.1038/nature13462
- 570 Zhou D. , Zhao S. , L. Zhang, G Sun and Y. Liu, 2015, The footprint of urban heat island effect in China, *Scientific*
571 *Reports*. 5: 11160
- 572 Zhou Y. , SmithS. , Zhao K. , M. Imhoff, A. Thomson, B. Lamberty,G. Asrar, X. Zhang, C. He and C. Elvidge, A
573 global map of urban extent from nightlights, *Env. Research Letters*, 10 (2015), (study uses a 2000 data set).

574
575
576

Conflicts of Interest

The author declares that he has no conflicts of interest.

578
580